

Spectral function of the Kondo model in high magnetic fields

A. Rosch, T. A. Costi, J. Paaske, and P. Wölfle

Institut für Theorie der Kondensierten Materie, Universität Karlsruhe, D-76128 Karlsruhe.

(Dated: January 29, 2020)

Using a recently developed perturbative renormalization group (RG) scheme, we calculate analytically the spectral function of a Kondo impurity for either large frequencies ω or large magnetic field B and arbitrary frequencies. For large $\omega \gg \max[B, T_K]$ the spectral function decays as $1/\ln^2[\omega/T_K]$ with prefactors which depend on the magnetization. The spin-resolved spectral function displays a pronounced peak at $\omega \sim B$ with a characteristic asymmetry. In a detailed comparison with results from numerical renormalization group (NRG) and bare perturbation theory in next-to-leading logarithmic order, we show that our perturbative RG scheme is controlled by the small parameter $1/\ln[\max(\omega, B)/T_K]$. Furthermore, we assess the ability of the NRG to resolve structures at finite frequencies.

PACS numbers: 72.15.Qm, 73.63.Kv, 75.20.Hr

I. INTRODUCTION

Only recently it has become possible to measure directly^{1,2,3} the so-called Kondo resonance, i.e. a sharp resonance characteristic for the spectral function of a single magnetic impurity in a metal. The Kondo resonance is probably the most direct manifestation of the Kondo effect⁴: The antiferromagnetic coupling between conduction electrons and a localized spin causes a complex many-body resonance which ultimately screens the magnetic degree of freedom. The spectral function is directly proportional to a tunneling current, e.g. from the tip of a scanning tunneling microscope to a magnetic impurity on the surface of a metallic host¹. Alternatively it can be measured by tunneling through weak links into a quantum dot in the Kondo regime^{2,3}. This also opens the possibility of investigating the spectral function out of equilibrium³.

While the spectral function is an interesting quantity in its own right, it also has many important applications. For example, it is directly related to the T -matrix, which describes the scattering of the conduction electrons (see below). It therefore determines not only the transport properties of magnetic impurities and quantum dots in the Kondo regime but it also plays an important role in controlling the distribution⁵ of electrons in metals contaminated by magnetic impurities. Furthermore, the spectral function of impurity models is central in determining the properties of lattice models within dynamical mean field theory⁶.

The spectral function of the Kondo model in a magnetic field has been calculated using a variety of techniques^{4,7,8,9,10,11,12,13,14,15}, including diagrammatics, mean-field treatments and quantum Monte-Carlo. The most precise method, however, is the numerical renormalization group¹⁶ (NRG) and its generalizations^{11,17,18,19} which allow the calculation of dynamical quantities. However, little is known analytically about the properties of the spectral function, particularly for high magnetic fields. For small B , the spectral function for small frequencies can be calculated from Fermi liquid theory

and renormalized perturbation theory^{13,14}. We have recently developed²⁰ a perturbative renormalization group scheme based on frequency-dependent couplings for the Kondo model. While this method was formulated to describe the Kondo effect out of equilibrium, it can also be used to calculate dynamical quantities in equilibrium in a controlled way for either large frequencies or large magnetic fields. We therefore use this method to determine analytically the spectral function in leading order of $1/\ln[\max(B, \omega)/T_K]$, focusing our attention on equilibrium and vanishing temperature. This clarifies some long-standing questions on the asymptotics of the spectral function in the Kondo model. A detailed comparison with results from NRG and with perturbation theory allows us to check the assumptions underlying our perturbative RG approach.

II. THE MODEL

We consider the spectral function $\text{Im}G_{\sigma}^f(\omega)$ of an electron in an impurity orbital within the Anderson model

$$H_A = \sum_{\mathbf{k}, \sigma} \varepsilon_{\mathbf{k}} c_{\mathbf{k}\sigma}^{\dagger} c_{\mathbf{k}\sigma} + \sum_{\sigma} \epsilon_f f_{\sigma}^{\dagger} f_{\sigma} + V \sum_{\mathbf{k}, \sigma} (c_{\mathbf{k}\sigma}^{\dagger} f_{\sigma} + h.c.) + U n_{f, \uparrow} n_{f, \downarrow} \quad (1)$$

where $c_{\mathbf{k}\sigma}^{\dagger}$ and f_{σ}^{\dagger} are creation operators for electrons in the conduction band and in the impurity orbital, respectively, $n_{f\sigma} = f_{\sigma}^{\dagger} f_{\sigma}$, and U is a large Coulomb interaction matrix element. We focus our attention on the Kondo regime, $\epsilon_f \ll -V^2 N_F$, $\epsilon_f + U \gg V^2 N_F$ (N_F being the conduction electron density of states), where the impurity orbital is occupied by a localized spin \mathbf{S} (with $S = 1/2$) and the problem can be mapped onto the Kondo Hamiltonian

$$H_K = \sum_{\mathbf{k}, \sigma} \varepsilon_{\mathbf{k}} c_{\mathbf{k}\sigma}^{\dagger} c_{\mathbf{k}\sigma} - B S_z + J \sum_{\mathbf{k}, \mathbf{k}', \sigma, \sigma'} \mathbf{S} \cdot c_{\mathbf{k}'\sigma'}^{\dagger} \boldsymbol{\tau}_{\sigma'\sigma} c_{\mathbf{k}\sigma}. \quad (2)$$

where $\boldsymbol{\tau}$ is the vector of Pauli matrices. Note, that we have coupled an extra magnetic field B to the impurity²¹, measuring B in units of the Zeeman splitting.

The Green function G_σ^f within the Anderson model is directly related to the T -matrix $T_\sigma(\omega) = V^2 G_\sigma^f(\omega)$ of the conduction electrons, defined by

$$g_{\sigma,\mathbf{k},\mathbf{k}'}^c(\omega) = g_{\mathbf{k}}^0(\omega)\delta(\mathbf{k} - \mathbf{k}') + g_{\mathbf{k}}^0(\omega)T_\sigma(\omega)g_{\mathbf{k}'}^0(\omega) \quad (3)$$

where $g_{\sigma,\mathbf{k},\mathbf{k}'}^c$ ($g_{\mathbf{k}}^0$) is the (bare) Green function of the conduction electrons. While it is not completely obvious how to define a spectral function for a Kondo impurity, the T -matrix of the Kondo model can easily be identified with the following correlation function, e.g. using equations of motion¹⁰,

$$T_\sigma(\omega) = V^2 G_\sigma^f(\omega) = J\langle S_z \rangle + J^2 \langle\langle \mathbf{S}c_\alpha^\dagger \boldsymbol{\tau}_{\alpha\sigma}; \mathbf{S}\boldsymbol{\tau}_{\sigma\alpha'} c_{\alpha'} \rangle\rangle, \quad (4)$$

where $\langle\langle \dots \rangle\rangle$ denotes a retarded correlation function. Formally, we will consider the usual ‘‘scaling limit’’, where the ratios of frequency or magnetic field and Kondo temperature, ω/T_K , B/T_K , are kept fixed while the ratio of T_K and all ‘‘high energy’’ scales like bandwidth D_0 , level position or interaction are sent to zero, $T_K/D_0, T_K/U, T_K/\epsilon_f \rightarrow 0$. In this limit, the dimensionless product of the T -matrix and the density of states, $N_F \text{Im}T(\omega)$, is a universal function of ω/T_K and B/T_K and it coincides with the low-frequency part of the spectral function $N_F V^2 \text{Im}G_\sigma^f(\omega)$ of the Anderson impurity. Therefore $N_F \text{Im}T_\sigma(\omega)$ is the quantity to be studied below.

III. PERTURBATIVE RG

The perturbation theory of the Kondo model is characterized by logarithmic divergences. The method of choice for the resummation of leading logarithmic corrections is the perturbative renormalization group (RG). In Ref. 20 we have developed a certain formulation of perturbative

RG based on frequency-dependent coupling constants. A thorough discussion of this approach will be published elsewhere²²; here we will use the RG equations without further derivation and check the results extensively in a comparison with bare perturbation theory and NRG.

The RG is formulated in terms of frequency- and spin-dependent vertices²³ $g_{\gamma\omega_f;\gamma'\omega'_f}^{\sigma\omega_c;\sigma'\omega'_c}$ where σ and ω_c (γ and ω_f) denote the spin and energy of the incoming electron (the incoming spin), see Ref. 20. Primed quantities refer to outgoing particles. Before renormalization starts, the vertex $g_{\gamma\omega_f;\gamma'\omega'_f}^{\sigma\omega_c;\sigma'\omega'_c}$ is just given by the bare coupling $N_F J \boldsymbol{\tau}_{\gamma\gamma'} \boldsymbol{\tau}_{\sigma\sigma'}$ independent of frequencies. In leading order of the relevant expansion parameter $1/\ln[\max(\omega, B)/T_K]$, one can set the energy of the spin on-shell $\omega_f = -\gamma B/2, \omega'_f = -\gamma' B/2$ to keep track only of the energy of the incoming electron. The vertex is parametrized as

$$g_{\gamma,-\gamma B/2;\gamma',-\gamma' B/2}^{\sigma,\omega;\sigma',\omega-(\gamma-\gamma')B/2} = \tau_{\gamma\gamma'}^z \tau_{\sigma\sigma'}^z \tilde{g}_{z\sigma}(\omega) + (\tau_{\gamma\gamma'}^x \tau_{\sigma\sigma'}^x + \tau_{\gamma\gamma'}^y \tau_{\sigma\sigma'}^y) \tilde{g}_\perp(\omega - \gamma B/2) \quad (5)$$

and the RG equations in terms of the running cut-off D read²⁰

$$\begin{aligned} \frac{\partial \tilde{g}_{z\sigma}(\omega)}{\partial \ln D} &= -2\tilde{g}_\perp(B/2)^2 \Theta(D - |\omega + \sigma B|) \\ \frac{\partial \tilde{g}_\perp(\omega)}{\partial \ln D} &= - \sum_{\sigma=-1,1} \tilde{g}_\perp\left(\frac{\sigma B}{2}\right) \tilde{g}_{z\sigma}(0) \Theta\left(D - \left|\omega + \frac{\sigma B}{2}\right|\right) \end{aligned} \quad (6)$$

with $\tilde{g}_\perp(\omega) = \tilde{g}_\perp(-\omega)$, $\tilde{g}_{z\uparrow}(\omega) = \tilde{g}_{z\downarrow}(-\omega)$ and the initial conditions $\tilde{g}_{z\sigma}(\omega) = \tilde{g}_\perp(\omega) = JN_F$ at the bare cut-off D_0 . The Theta function $\Theta(\omega)$ describes that various virtual processes are not possible if the running cut-off D gets too small. Note that one recovers the usual poor man’s scaling equations²⁴ if one considers only the limit $\omega \rightarrow 0$ as it is usually done in RG schemes.

The RG equations (6) are easily solved and we obtain for $D \rightarrow 0$

$$\begin{aligned} \tilde{g}_{z\sigma}(\omega) &= \Theta[|\omega + \sigma B| - B] \frac{1}{2 \ln[|\omega + \sigma B|/T_K]} + \Theta[B - |\omega + \sigma B|] \frac{1}{2 \ln[B/T_K]} \left| \frac{B}{\omega + \sigma B} \right|^{1/\ln[B/T_K]} \\ \tilde{g}_\perp(\omega) &= \sum_\sigma \Theta[|\omega + \sigma \frac{B}{2}| - B] \frac{1}{4 \ln[|\omega + \sigma \frac{B}{2}|/T_K]} + \Theta[B - |\omega + \sigma \frac{B}{2}|] \left(\frac{1}{2 \ln[B/T_K]} \left| \frac{B}{\omega + \sigma \frac{B}{2}} \right|^{\frac{1}{2 \ln[B/T_K]}} - \frac{1}{4 \ln[B/T_K]} \right) \end{aligned} \quad (7)$$

where within our one-loop approach $T_K = D_0 e^{-1/(2N_F J)}$. As expected, the dimensionless renormalized couplings are functions of ω/T_K and B/T_K only.

It is important to realize that the logarithmic renor-

malizations resummed in Eq. (6) are finally cut off by the relaxation rate Γ of the spin. As the relevant processes involve at least one spin-flip, we identify Γ with the transverse spin relaxation rate $1/T_2$, which is given

in terms of the renormalized couplings as²⁰

$$\Gamma = \frac{\pi}{4} \sum_{\gamma=-1,1} \int d\omega \left[\tilde{g}_{z\gamma}(\omega)^2 f_\omega(1-f_\omega) + \tilde{g}_\perp(\omega - \gamma B/2)^2 f_\omega(1-f_{\omega-\gamma B}) \right]. \quad (8)$$

where f_ω is the Fermi function. The rate Γ cuts off the power-law singularities at $\omega = \pm B$ (or $\omega = \pm B/2$) and we implement this by replacing $B/|\omega + \sigma B|$ by $\sqrt{\Gamma^2 + B^2}/\sqrt{\Gamma^2 + (\omega + \sigma B)^2}$ in (7). The errors introduced by this heuristic replacement are small²² in $1/\ln[\max(B, \omega)/T_K]$. For $B \gg T_K$, we obtain $\Gamma \approx \pi B/(16 \ln^2[B/T_K]) \gg T_K$ and therefore $\tilde{g}_{z\sigma}(\omega) \ll 1$ and

$$\tilde{g}_\perp(\omega) \approx g + g^2 \left(\ln \frac{D_0}{|\omega - \frac{B}{2}|} + \ln \frac{D_0}{|\omega + \frac{B}{2}|} \right) + \frac{g^3}{2} \left(\ln^2 \frac{D_0}{|\omega - \frac{B}{2}|} + 6 \ln \frac{D_0}{|\omega - \frac{B}{2}|} \ln \frac{D_0}{|\omega + \frac{B}{2}|} + \ln^2 \frac{D_0}{|\omega + \frac{B}{2}|} \right) \quad (9)$$

$$\tilde{g}_{z\sigma}(\omega) \approx g + 2g^2 \ln \frac{D_0}{|\omega + \sigma B|} + 2g^3 \left(\ln \frac{D_0}{|\omega|} \left[\ln \frac{D_0}{|\omega + \sigma B|} - \ln \frac{D_0}{B} \right] + \ln \frac{D_0}{|\omega + \sigma B|} \left[\ln \frac{D_0}{|\omega + \sigma B|} + \ln \frac{D_0}{B} \right] \right), \quad (10)$$

where $g = N_F J$. The perturbative RG is expected to resum *all* leading logarithmic terms. Indeed, if we expand (7) carefully in g using that $T_K = D_0 e^{-1/(2g)}$, we obtain the same logarithmic divergences in all relevant limits, $\omega \rightarrow \pm B/2$ or $\omega \rightarrow \pm B$, $\omega \rightarrow \pm \infty$, and $\omega \rightarrow 0$ [the singularity at $\omega = 0$ in (10) cancels]. One assumption which has not been checked in the perturbative calculation shown above is that the logarithms are cut off by the spin-relaxation rate. To analyze this effect one would have to include self-energy insertions and corresponding vertex corrections as will be discussed in a future publication²².

To leading order in $1/\ln[\max(\omega, B)/T_K]$ the spectral function can be calculated by replacing the bare coupling constants in the lowest order expression (inset of Fig. 2) with the renormalized vertex (5) and one obtains²⁶

$$N_F \text{Im}[T_\sigma(\omega)] = -\frac{\pi}{4} \left(\tilde{g}_{z\sigma}(\omega)^2 + 2\tilde{g}_\perp(\omega + \sigma \frac{B}{2})^2 [1 + \sigma M(2f_\Gamma(\omega + \sigma B) - 1)] \right) \quad (11)$$

where $M = 2\langle S_z \rangle$ is the magnetization of the impurity normalized to 1. The Fermi function $f_\Gamma(\omega \pm B)$ has to be broadened by Γ , $f_\Gamma(\omega) = 1/2 - \arctan[\omega/\Gamma]/\pi$. Diagrammatically this arises as the corresponding term in $T(\omega)$ contains a convolution with the spin-flip susceptibility $\chi^{+-}(\omega)$ (see inset of Fig. 2) and we used the fact that the ω -dependence of the vertex $\tilde{g}_\perp(\omega)$ is sufficiently weak.

For $B \gg T_K$ one can replace M in (11) by 1 in leading order of $1/\ln[B/T_K]$. However, to obtain the correct large- ω behavior for arbitrary B it is essential to use the exact local magnetization. For $B \sim T_K$ it is not possible

$\tilde{g}_\perp(\omega) \ll 1$. Accordingly, the perturbative RG is valid in this regime²⁵ for *all* frequencies (while for $B \lesssim T_K$ it can be used only for $\omega \gg T_K$). The smallness of the renormalized couplings for either large B or large ω is the main reason why our calculation is controlled by $1/\ln[\max(\omega, B)/T_K]$ as e.g. higher-order corrections to (6) remain small.

To check the assumptions underlying our formulation of the perturbative RG for ω -dependent vertices, we have calculated the vertices in next-to-leading logarithmic order in bare perturbation theory by evaluating the diagrams shown in Fig. 1. Such a test seems to be useful as RG schemes for ω -dependent vertices are not used very often. Neglecting terms of order $g^3 \ln D_0$, we obtain

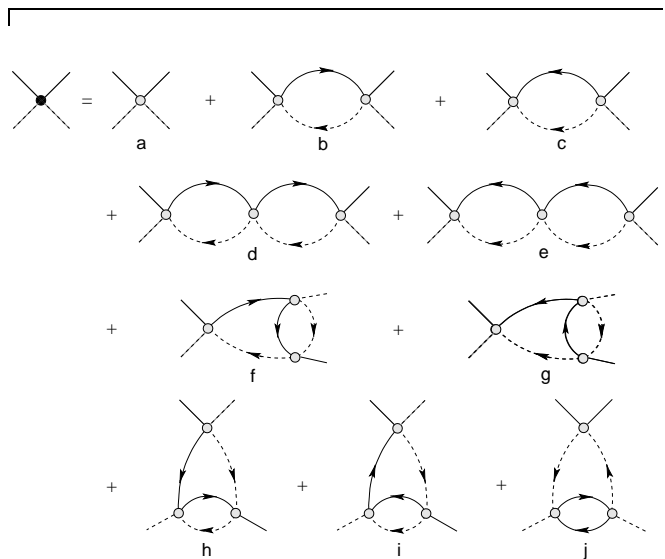


FIG. 1: Diagrams contributing to the vertex renormalization up to order g^3 . Solid line: conduction electrons, dashed line: pseudo fermions representing the spin. See [20] for the corresponding Feynman rules. The (non-parquet) diagram (j) does not contribute to order $g^3 \ln^2 D_0$.

to calculate M within our RG scheme, and we therefore use the magnetization obtained from the Bethe Ansatz (or the practically identical values from the NRG).

Friedel's sum rule²⁷ relates the spectral function at $\omega = 0$ exactly to the local magnetization $N_F \text{Im}[T_\sigma(\omega = 0)] = -\frac{1}{\pi} \sin^2 \delta_\sigma$ where $\frac{\delta_\sigma}{\pi} = \frac{1 + \sigma M}{2}$. As a further check of our approach, we compare this result to our perturbative RG. From Eqs. (7) and (11), we obtain asymptotically

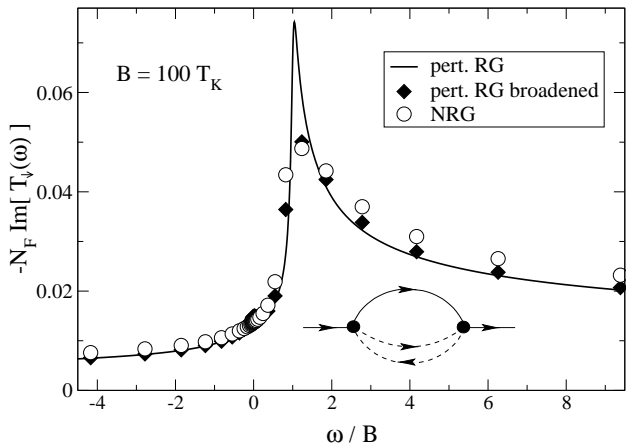


FIG. 2: T -Matrix $-N_F \text{Im}[T_{\downarrow}(\omega)]$ (or equivalently the spectral function $-N_F V^2 \text{Im}G_{\downarrow}^f(\omega)$ of an Anderson impurity) as a function of ω/B for $B = 100 T_K$. Solid line: perturbative RG, open circles: NRG. The NRG is not able to resolve sharp peaks at high frequencies. For a direct comparison, we have therefore convoluted (filled diamonds) the result of the perturbative RG with the resolution function used in the NRG code. Inset: Diagram used to calculate the T -matrix (4) in leading order using renormalized vertices.

$N_F \text{Im}[T_{\sigma}(\omega = 0)] \approx -\frac{\pi}{16} \frac{1}{\ln^2[B/T_K]}$ for $B \gg T_K$ which is consistent with the asymptotic Bethe Ansatz²⁸ result $M = 1 - 1/(2 \ln[B/T_K]) - \dots$

A typical spectral function for a spin-down electron is shown in Fig. 2; the corresponding spin-up spectral function can be obtained from $\text{Im}T_{\uparrow}(\omega) = \text{Im}T_{\downarrow}(-\omega)$. For large frequencies the spectral function decays as

$$N_F \text{Im}[T_{\sigma}(\omega)] \approx -\pi \frac{3 \mp 2\sigma M}{16 \ln^2[\omega/T_K]} \quad \text{for } \omega \rightarrow \pm\infty. \quad (12)$$

A similar result, discussed below, has been obtained by Logan and Dickens^{13,29}.

For $\omega \sim B$ the spectral function is characterized by a pronounced and highly asymmetric peak. The width of the left flank is determined by Γ and is therefore of order $B/\ln^2[B/T_K]$. As $\Gamma/B \sim 1/\ln^2[B/T_K]$ decreases for increasing B , the left flank sharpens with increasing B (see Fig. 3). As the width of the right flank increases for large B the peak gets more and more asymmetric. Formally, the line shape of the right flank is characterized by a power-law for $\Gamma \ll \omega - B \ll B$, see Eq. (7). However, the corresponding exponents α of order $1/\ln[B/T_K]$ are so small that it is not even in principle possible to extract the power-law behavior³⁰ as $\alpha \ln[B/\Gamma] \sim \ln[\ln(B/T_K)]/\ln(B/T_K) \ll 1$.

Within our perturbative RG, the peak in the spectral function is always positioned at $\omega = B$, see Fig. 3. This is the correct $B \rightarrow \infty$ result. A subleading shift towards lower values is not included in our scheme which neglects renormalization of the real part of the self-energy³¹. An estimate²² suggests that this effect is of order $B/\ln[B/T_K]$ consistent with results from Moore

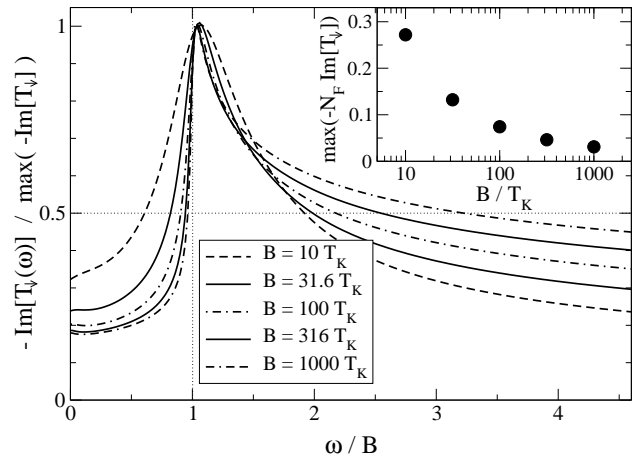


FIG. 3: Line shape of the spectral function as a function of ω/B calculated within perturbative RG. All curves are rescaled by their maximum. For increasing B the peaks get more and more asymmetric. Note that a small systematic shift of the peak position towards lower frequencies for smaller B is not included (see text). Inset: peak height as a function of B/T_K .

and Wen¹² discussed below. For $B \ll T_K$ it has been shown^{13,14,32} that the peak in the spectral function is positioned at $2B/3$. A splitting in the total spectral function $\text{Im}T_{\uparrow}(\omega) + \text{Im}T_{\downarrow}(\omega)$ can be observed¹⁰ for $B \gtrsim 0.5 T_K^*$, where $T_K^* \approx 2.8 T_K$ is the half width at half maximum (HWHM) of the Kondo resonance at $T = 0$.

IV. NRG

The results of the perturbative RG approach to the equilibrium T -matrix $T(\omega)$ can be compared to numerical renormalization group (NRG) results for the same quantity¹⁰. The NRG procedure¹⁶ consists of the following steps: (i) a logarithmic mesh of k -points $k_n = \Lambda^{-n}$ is introduced about the Fermi wavevector $k_F = 0$, and (ii) a unitary transformation of the $c_{k\sigma}$ is performed such that $f_{0\sigma} = \sum_k c_{k\sigma}$ is the first operator in a new basis, $f_{n\sigma}, n = 0, 1, \dots$, which tridiagonalizes $H_c = \sum_{k\sigma} \epsilon_{k\sigma} c_{k\sigma}^\dagger c_{k\sigma}$ in k -space, i.e. $H_c \rightarrow \sum_{\sigma} \sum_{n=0}^{\infty} \Lambda^{-n/2} (f_{n+1\sigma}^\dagger f_{n\sigma} + h.c.)$. The Hamiltonian (2) with the above discretized form of the kinetic energy is now iteratively diagonalized by defining a sequence of finite size Hamiltonians $H_N = \sum_{\sigma, n=0}^{N-1} \Lambda^{-n/2} (f_{n+1\sigma}^\dagger f_{n\sigma} + h.c.) + J \sum_{\sigma, \sigma'} \mathbf{S} \cdot f_{0, \sigma'}^\dagger \boldsymbol{\tau}_{\sigma' \sigma} f_{0, \sigma} - B S_z$ for $N \geq 0$. For each N , this yields the excitation energies E_{λ}^N and many-body eigenstates $|\lambda\rangle_N$ of H_N at a corresponding set of energy scales ω_N defined by the smallest scale in H_N , $\omega_N = \Lambda^{-\frac{N-1}{2}}$. Since the number of states grows as 4^N , for $N > 6$ only the lowest 500 or so states are retained for H_N . This limits the width of the spectrum of H_N to $0 \leq \omega \leq K(\Lambda)\omega_N$, where $K(\Lambda) \approx 5$ for the value $\Lambda = 1.5$ used in this paper. We are inter-

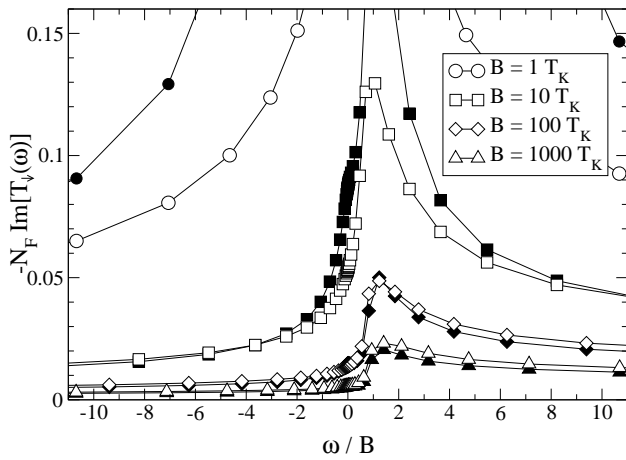


FIG. 4: Comparison of NRG (open symbols) and perturbative RG (filled symbols) broadened by the NRG-resolution function (see caption of Fig. 2) for large magnetic fields, $B = 1, 10, 100, 1000 T_K$.

ested in $\text{Im}T(\omega) = \text{Im}\langle\langle O; O^\dagger \rangle\rangle_\rho$, where $O = \mathbf{S}c_\alpha^\dagger \tau_{\alpha\sigma}$ is defined in Eq. (4) and the subscript ρ indicates the density matrix used to evaluate the thermodynamic averages (see below). The matrix elements $\langle m|O|n\rangle_N$, which are required for $T(\omega)$, are also calculated iteratively. $\text{Im}T(\omega)$ is then constructed at a characteristic set of frequencies $\omega = \Omega_N$ from H_N for each $N = 0, 1, \dots$ via its Lehmann representation. This necessarily yields $\text{Im}T(\omega)$ in the form of a set of weighted delta functions $\delta(\Omega_N \pm E_\lambda^N)$. Continuous spectra are obtained by replacing the delta functions by Gaussians of width η_N : $\delta(\Omega_N \pm E_\lambda^N) \rightarrow \frac{1}{\eta_N \sqrt{\pi}} \exp(-(\Omega_N \pm E_\lambda^N)^2 / \eta_N^2)$. As noted above, the spectrum of H_N is known in a finite window of size $\approx 5\omega_N$ for $\Lambda = 1.5$. We therefore choose $\Omega_N = 1.8\omega_N$, not too low since the lower part of the spectrum is refined in later iterations and not too close to the upper bound of the spectrum which could be subject to truncation errors. We also set $\eta_N = 0.39\Omega_N$ of order the level structure of H_N . The main interest in this paper is to compare the NRG results for $\text{Im}T(\omega, B, T = 0)$ with the perturbative RG calculations in the limit $B \gg T_K$ where the latter are expected to be accurate. In this limit, the spectral features in $\text{Im}T(\omega, B, T = 0)$ lie at high frequencies $\omega \approx B$. A description of this finite-field, high-frequency part of the spectrum within NRG requires the use of a reduced density matrix^{11,32} calculated from the true ground state, i.e. $H_{N \rightarrow \infty}$, in place of the grand-canonical density matrix obtained from H_N . The necessity to use ground-state properties to calculate high-frequency features is for example evident from Eq. (12): the magnetization determines the large- ω tails. Nevertheless, the two approaches have been shown to give almost identical results at $B = 0$ and to be in good agreement³² for fields $B \lesssim 10T_K$.

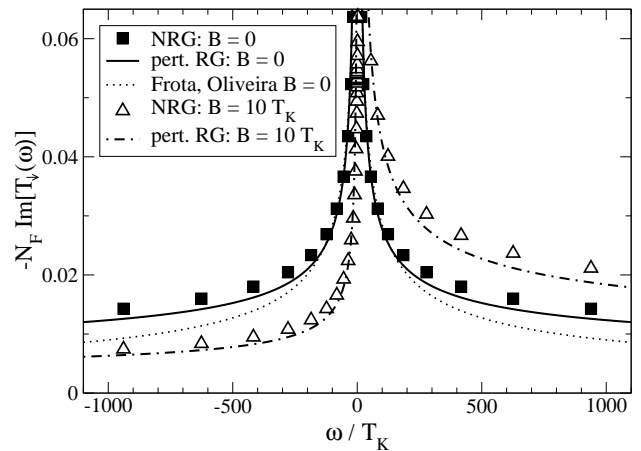


FIG. 5: Behavior of the spectral function $-N_F \text{Im}[T_\downarrow(\omega)] = -N_F V^2 \text{Im}G_\downarrow^f(\omega)$ for large ω and $B = 0, 10 T_K$. For $B, T_K \ll \omega$ the spectral function decays as $1/\ln^2[\omega/T_K]$ with prefactors depending on the magnetization [see Eq. (11)]. Symbols: NRG, solid and dot-dashed line: perturbative RG. For very large $\omega > 200 T_K$ one can see that an interpolation formula suggested in Ref. 17 (dotted line) decaying as $1/\sqrt{\omega}$ is not consistent²⁹ with the NRG data.

V. COMPARISONS

How well does the perturbative RG reproduce the spectral functions calculated within NRG? Fig. 2 shows excellent agreement³³ for $B/T_K = 100$ both for $\omega \rightarrow 0$ and $\omega \rightarrow \pm\infty$. However, large deviations arise for $\omega \approx B$ where the peak within the perturbative RG is much sharper and higher. This disagreement arises because the NRG cannot always resolve sharp features at high frequencies due to the logarithmic discretization in energy. More precisely, for a feature at a given frequency Ω_0 with intrinsic width Δ_0 it will fail to resolve it³⁴ if $\Omega_0 > \Delta_0$ since the broadening used at frequency Ω_0 is necessarily of order Ω_0 ($0.39\Omega_0$ in our calculations). This is the case here, since the spectral feature at $\Omega_0 = B$ has a width on its left flank given by $\Delta_0 \sim B/\ln^2[B/T_K]$. Consequently, the width of this feature will not be captured by NRG for $B \gg T_K$. To allow a direct comparison of NRG and perturbative RG, we have broadened the latter at the energy ω by convolution with the resolution function used in the NRG code, i.e. by a Gaussian of width 0.39ω . After this broadening, the agreement of perturbative RG and NRG is excellent for all frequencies as long as $B \gg T_K$, see Figs. 2 and 4. For smaller B , the spectral function cannot be calculated reliably for small ω within our perturbative RG and indeed strong deviations can be seen in Fig. 4 for $B \lesssim 10T_K$. Fig. 5 shows that the large ω behavior is nevertheless well reproduced which firmly establishes Eq. (12). Note that we replaced M in (11) by the true ground-state magnetization for this comparison as discussed above.

We have argued that the small parameter con-

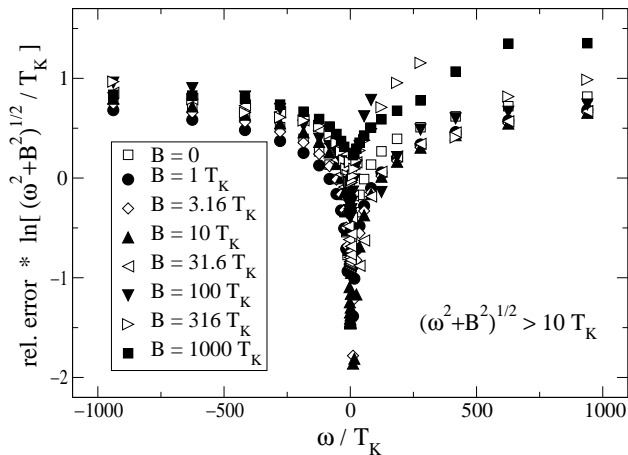


FIG. 6: The perturbative RG is a controlled expansion in the small parameter $1/\ln[\max[\omega, B]/T_K]$. This is shown by plotting the relative error of the perturbative RG compared to NRG, $\frac{\text{NRG-pert.RG}}{\text{NRG}}$, multiplied by $\ln[\sqrt{\omega^2 + B^2}/T_K]$ for various frequencies and magnetic fields. The perturbative RG results have been broadened by the NRG resolution (see Fig. 2 and text). Only data points with $\sqrt{\omega^2 + B^2} > 10T_K$ are shown.

trolling the validity of our perturbative RG is $1/\ln[\max(B, \omega)/T_K]$. To check this claim we plot in Fig. 6 the relative error of the perturbative RG (compared to NRG) multiplied by $\ln[\sqrt{\omega^2 + B^2}/T_K]$ for a wide range of ω and B . As expected, one obtains a number of order unity! Fig. 6 suggests that the next-order correction is suppressed by a factor smaller than $1.5/\ln[\max(B, \omega)/T_K]$. From the large- B expansion of quantities like the magnetization calculated by Bethe Ansatz^{4,28} one expects that the correction rather has the form $\ln[\ln[\max(B, \omega)/T_K]]/\ln[\max(B, \omega)/T_K]$ but our range of parameters is too small to extract a $\ln[\ln[\dots]]$ prefactor.

In the remainder of this section, we briefly compare our results to other approaches. Many years ago, Frota and Oliveira¹⁷ described the spectral function for $B = 0$ with the simple heuristic form $N_F T(\omega) = -1/\text{Re}[\pi(1 - i\omega/\Gamma_K)^{1/2}]$ where $\Gamma_K \approx 0.4T_K$ (in our units) was fitted to the width of the Kondo peak. This form was chosen to interpolate between the exact $\omega = 0$ result and an asymptotic $1/\sqrt{\omega}$ behavior which was believed to arise as a consequence of an X-ray singularity in the presence of a phase-shift $\pi/2$. The fit to the Frota and Oliveira formula works surprisingly well for frequencies up to $200T_K$ (see Fig. 5). From our point of view, this remarkable agreement is, however, accidental in the following sense: For $T_K \ll \omega \ll D$ the spectral function decays as $1/\ln^2[\omega/T_K]$ and not as $1/\sqrt{\omega}$ as has previously been pointed out by Dickens and Logan²⁹. Does a $1/\sqrt{\omega}$ law hold at intermediate frequencies, e.g. for $T_K \ll \omega \ll T^*$? This would require the existence of a new scale T^* parametrically larger than T_K in contra-

dition not only to the perturbative RG but also to the exact Bethe Ansatz solution²⁸. Nevertheless, the Frota-Oliveira formula is a very good heuristic description in a large regime. For $20T_K < \omega < 200T_K$ it is almost indistinguishable from our perturbative RG result for $B = 0$ (and fits the exact result much better for $\omega < 20T_K$ where our perturbative scheme breaks down).

Recently, Logan and Dickens^{13,29} calculated the spectral functions in a magnetic field within their “local moment approach” (LMA), which is based on a combination of diagrammatic perturbation theory and mean-field theory. Interestingly, Logan and Dickens obtain the correct $\omega \rightarrow \infty$ and $\omega \rightarrow 0$ asymptotics. However the peak in the spectral function close to $\omega = B$ appears to be much broader in their approach and they find that the peak is shifted towards larger frequencies of order $B \ln(B/T_K)$. We think that both features are an artifact of their heuristic scheme to introduce broadening.

Moore and Wen¹² calculated the density of states of the spinons obtained from the Bethe Ansatz solution²⁸. They suggested that their result may serve as an approximation to the spectral function. However, the spinon density of states lacks the logarithmic tails characterizing the large ω behavior of the spectral function and their peaks close to $\omega = B$ do not show the correct asymmetric line shape for $B \gg T_K$. Nevertheless, it is interesting to note that the width of the spinon density of states is of order $\sim B/\ln^2[B/T_K]$ like the left flank of our result. In their result, the position of the peak in the spectral function is shifted by $-B/(2 \ln[B/T_K])$ away from $\omega = B$ for $B \gg T_K$. As discussed above, such a shift is beyond the precision of our present calculation but an interesting open question is whether the peak-position in the spinon density of states coincides with that in the electron spectral function.

VI. CONCLUSION

In this paper we have addressed three problems in particular.

(i) We have calculated analytically the behavior of the universal spectral function in the Kondo model for either large frequencies or large magnetic field and arbitrary frequencies. We hope that our results establishes the existence and detailed shape of the highly asymmetric peak at frequencies of the order of the Zeeman splitting and the asymptotic behavior at high frequencies. Hopefully, the spectral function in a magnetic field can be studied in some detail in future experiments e.g. by tunneling into magnetic impurities.

(ii) In a detailed comparison with perturbation theory and NRG, we have argued that our recently developed perturbative RG scheme²⁰ allows controlled calculations in the small parameter $1/\ln[\max(\omega, B)/T_K]$. We expect that a similar statement holds out of equilibrium for large bias voltages $V \gg T_K$ where a comparison with numerically exact results is not yet possible.

(iii) We have tried to assess the ability of the NRG to resolve structures at high frequencies. As is obvious from the formulation of NRG, structures which are much sharper than their typical frequency are not correctly reproduced by NRG. However, our results suggest that the error induced by the logarithmic discretization mainly results in a simple broadening. This may have some relevance for recent implementations of dynamical mean field theory using NRG³⁵. The spectral function for large B can serve as a test for future improvements of the NRG

algorithms adapted to describe high- ω features more precisely.

We thank J. Kroha, D.E. Logan, J. Martinek and M. Vojta for helpful discussions and especially L. Glazman who motivated us to check the validity of our RG approach in more detail. This work was supported in part by the CFN, the Emmy Noether program (A.R.) of the DFG and the SFB 195 of the DFG (TAC). We also thank the Ørsted Laboratory for hospitality during parts of this work (J.P.).

-
- ¹ J. Li, W.-D. Schneider, R. Berndt, and B. Delley, Phys. Rev. Lett. **80**, 2893 (1998), V. Madhavan, W. Chen, T. Jamneala, M. F. Crommie, and N. S. Wingreen, Science **280**, 567 (1998); H. C. Manoharan, C. P. Lutz, and D. W. Eigler, Nature **403**, 512 (2000). N. Knorr, M. A. Schneider, L. Diekhöner, P. Wahl, and K. Kern, Phys. Rev. Lett. **88**, 096804 (2002).
- ² D. Goldhaber-Gordon *et al.*, Nature **391**, 156 (1998); S. M. Cronenwett, T. H. Oosterkamp and L. P. Kouwenhoven, Science **281**, 540 (1998); W. G. van der Wiel *et al.*, Science **289**, 2105 (2000); J. Nygård, D. H. Cobden and P. E. Lindelof, Nature **408**, 342 (2000).
- ³ S. De Franceschi *et al.*, Phys. Rev. Lett. **89**, 156801 (2002).
- ⁴ A. C. Hewson, *The Kondo Problem to Heavy Fermions*, Cambridge University Press (1993).
- ⁵ J. Kroha, Adv. Solid State Phys. **40**, 216 (2000); A. Kaminski, L. I. Glazman, Phys. Rev. Lett. **86**, 2400 (2001); G. Göppert and H. Grabert, Phys. Rev. B **64**, 033301 (2001); J. Kroha and A. Zawadowski, Phys. Rev. Lett. **88**, 176803 (2002).
- ⁶ W. Metzner and D. Vollhardt, Phys. Rev. Lett. **62**, 324 (1989); A. Georges, G. Kotliar, W. Krauth, and M. J. Rozenberg, Rev. Mod. Phys. **68**, 13 (1996).
- ⁷ Y. Meir, N. S. Wingreen, and P. A. Lee, Phys. Rev. Lett. **70**, 2601 (1993).
- ⁸ O. Sakai, S. Suzuki, W. Izumida, and A. Oguri, J. Phys. Soc. Jap. **68**, 1640 (1999).
- ⁹ O. Takagi and T. Saso, J. Phys. Soc. Jap. **68**, 1997 (1999).
- ¹⁰ T. A. Costi, Phys. Rev. Lett. **85**, 1504 (2000).
- ¹¹ W. Hofstetter, Phys. Rev. Lett. **85**, 1508 (2000).
- ¹² J. E. Moore and X. G. Wen, Phys. Rev. Lett. **85**, 1722 (2000).
- ¹³ D. E. Logan and N. L. Dickens, Europhys. Lett. **54**, 227 (2001), D. E. Logan and N. L. Dickens, J. Phys.: Cond. Mat. **13**, 9713 (2001).
- ¹⁴ A. C. Hewson, J. Phys.: Cond. Mat. **13**, 10011 (2001).
- ¹⁵ J. Martinek *et al.*, preprint cond-mat/0210006.
- ¹⁶ K. G. Wilson, Rev. Mod. Phys. **47**, 773 (1975); H. R. Krishna-murthy, J. W. Wilkins and K. G. Wilson, Phys. Rev. **B21**, 1003 (1980).
- ¹⁷ H. O. Frota and L. N. Oliveira, Phys. Rev. B **33**, R7871 (1986).
- ¹⁸ O. Sakai, Y. Shimizu and T. Kasuya, J. Phys. Soc. Jap. **58** 3666 (1989)
- ¹⁹ T. A. Costi, A. C. Hewson and V. Zlatić, J. Phys. Cond. Mat. **6** 2519 (1994).
- ²⁰ A. Rosch, J. Paaske, J. Kroha and P. Wölfle, accepted for publication in PRL, cond-mat/0202404.
- ²¹ Adding a magnetic field also to the conduction electrons will not change the results in the scaling limit as the density of states of the up and down electrons at the Fermi energy remains independent of B .
- ²² A. Rosch, J. Paaske, J. Kroha, P. Wölfle, unpublished.
- ²³ The vertices are defined using a pseudo spin representation of the spin, see Ref. 20.
- ²⁴ P. W. Anderson, J. Phys. C **3**, 2436 (1966).
- ²⁵ A. Rosch, J. Kroha and P. Wölfle, Phys. Rev. Lett. **87**, 156802 (2001).
- ²⁶ While we are considering only equilibrium quantities, the proper replacements of bare and renormalized quantities is most easily done in the Keldysh formulation where it is easy to identify correctly the impurity magnetization in (11). In an equilibrium technique it would be far from obvious that $\tanh(B/2T)$ has to be replaced by M .
- ²⁷ D. C. Langreth, Phys. Rev. **150**, 516 (1966); P. Nozières, J. Low Temp. Phys. **17**, 31 (1974).
- ²⁸ N. Andrei, Phys. Rev. Lett. **45**, 379 (1980); N. Andrei, Phys. Lett. **87A**, 299 (1982).
- ²⁹ N. L. Dickens and D. E. Logan, J. Phys.: Cond. Mat. **13**, 4505 (2001).
- ³⁰ To extract a power law $x^\alpha = e^{\alpha \ln x}$ the variations of the argument of the e function should be large compared to 1.
- ³¹ M. Salmhofer and C. Honerkamp, Prog. Theo. Physics **105**, 1 (2001).
- ³² T. A. Costi, proceedings of NATO ARW on “Concepts in Electron Correlations”, Hvar, Croatia (2002), cond-mat/0212651.
- ³³ For our NRG results we use the asymptotically exact two-loop definition $T_K = D_0 \sqrt{2N_F J} e^{-1/(2N_F J)}$ of the Kondo temperature to be identified with $T_K = D_0 e^{-1/(2N_F J)}$ within our one-loop perturbative RG.
- ³⁴ T. A. Costi, in *Density Matrix Renormalization*, edited by I. Peschel, X. Wang, M. Kaulke and K. Hallberg (Springer, Berlin, Germany 1999).
- ³⁵ R. Bulla, Phys. Rev. Lett. **83**, 136 (1999); R. Bulla, T. A. Costi and D. Vollhardt, Phys. Rev. B **64**, 045103 (2001); R. Zitzler, Th. Pruschke and R. Bulla, Eur. Phys. J. B **27**, 473 (2002); T. A. Costi and N. Manini, J. Low Temp. Phys. **126**, 835 (2002).